

MIT Open Access Articles

*Selective Recovery of Gold from E-Wastewater Using Poly-*m*-phenylenediamine Nanoparticles and Assembled Membranes*

The MIT Faculty has made this article openly available. **Please share** how this access benefits you. Your story matters.

Citation: Chen, Yuchao, Wang, Li, Shu, Yufei, Han, Qi, Chen, Beizhao et al. 2023. "Selective Recovery of Gold from E-Wastewater Using Poly-*m*-phenylenediamine Nanoparticles and Assembled Membranes." ACS Applied Engineering Materials, 1 (8).

As Published: 10.1021/acsaenm.3c00259

Publisher: American Chemical Society (ACS)

Persistent URL: <https://hdl.handle.net/1721.1/153825>

Version: Author's final manuscript: final author's manuscript post peer review, without publisher's formatting or copy editing

Terms of use: Creative Commons Attribution-Noncommercial-ShareAlike



Selective Recovery of Gold from E-wastewater Using Poly-m-phenylenediamine Nanoparticles and Assembled Membrane

Yuchao Chen^{a,1}, Li Wang^{a,1}, Yufei Shu^a, Qi Han^a, Beizhao Chen^a, Mengxia Wang^a,
Xun Liu^a, Danyal Rehman^b, Bei Liu^{a*}, Zhongying Wang^{a*}, John Lienhard^b

^a School of Environmental Science and Engineering, Southern University of Science and
Technology, Shenzhen 518055, China

^b Department of Mechanical Engineering, Massachusetts Institute of Technology, Cambridge
MA 02139, USA

2023

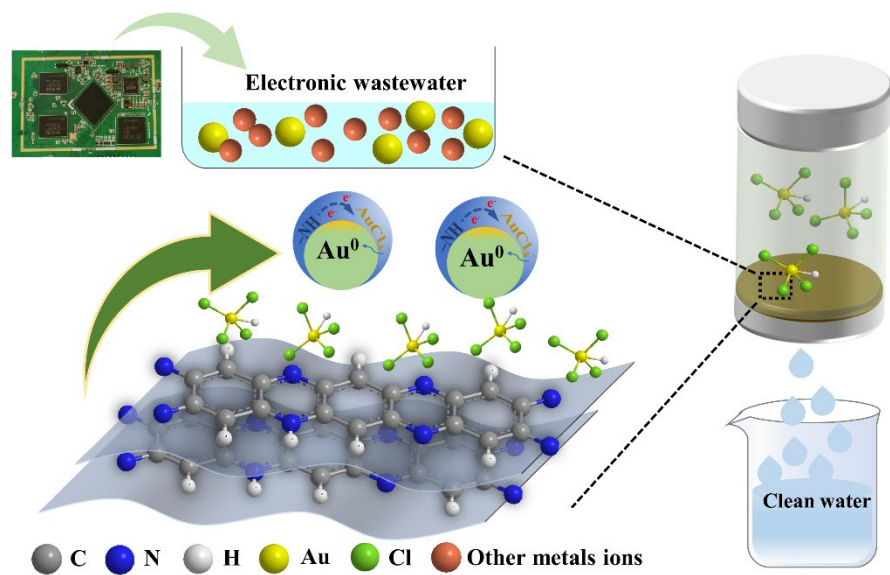
* to whom correspondence should be addressed. e-mail: liub@sustech.edu.cn; wangzy6@sustech.edu.cn.

Abstract

The economic value of recovering gold from electronic waste (e-waste) has generated significant interest, but selective capture of gold from complex acidic electronic leaching solutions remains challenging. Here, we synthesized Poly-m-phenylenediamine (PmPD) nanoparticles with a positively charged surface and amino functional groups, resulting in an adsorption capacity of 2063 mg/g for Au(III) in acidic solutions, superior to most traditional adsorbents. Electrostatic adsorption and reduction were identified as the adsorption mechanism for Au(III) by zeta potential, XRD, TEM, FT-IR, and XPS analyses. To enable adsorbent recycle, PmPD nanoparticles were assembled into adsorptive membranes and used for gold recovery from e-wastewater *via* a continuous-flow membrane separation process. The PmPD membrane achieved a dynamic gold recovery capacity of approximately 530 mg/g and could be effectively regenerated after washing with a mixture of thiourea and HCl. We demonstrated the practical application of the adsorptive membranes by recovering about 100% of gold from the leaching solution of waste printed circuit boards of computers. Finally, the recovered gold nanoparticles on PmPD membrane were used to catalyze the degradation of *p*-nitrophenol, showcasing the catalytic property of gold. The Au@PmPD membrane loaded with 4 mg gold exhibited a high catalytic reduction performance with an apparent rate constant of 0.59 min^{-1} , one of the highest catalytic degradation rate constants of *p*-nitrophenol reported to date. Our study presents an effective and economical approach for recovering gold from e-waste, providing a prototype of resource recovery and reuse.

Keywords: polyaniline; gold recovery; selective adsorption; membrane; electronic wastewater

Table of Contents (TOC) and Abstract Art



Introduction

The precious metal gold (Au) is widely utilized in the electronic industry due to its excellent conductivity,¹ corrosion resistance,² and ductility.³ The rapid development of the electronic industry has led to an ever-increasing demand for gold, with a reported global demand of 330 tons in 2021.⁴ However, as a scarce resource, the limited supplies of gold from ore mining cannot meet the consumption demand.⁵ On the other hand, the growth of the industry has also resulted in the generation of over 53.6 million tons of electronic waste (e-waste) worldwide each year,⁶ leading to severe gold loss. It has been reported that one ton of waste printed circuit boards (WPCBs) contains about 80–1500 g of gold, which is 4–800 times higher than that in gold ore.⁷ Therefore, gold recycling from e-waste has emerged as an alternative way to produce gold besides ore mining.⁸ The recovery of gold from e-waste is a crucial goal in turning trash into treasure, as it aims to reduce environmental pollution while recycling the precious metal.

The e-waste is commonly pretreated through mechanical separation and chemical reagents to produce e-wastewater for further treatment. Over the past two decades, hydrometallurgical approaches have been extensively applied to the recovery of gold from e-waste.⁹ Hydrometallurgical processes are often performed with acid (cyanide (CN^-) or thiosulfate ($\text{S}_2\text{O}_3^{2-}$)) or caustic leaching of e-waste, followed by separation and recovery procedures such as chemical precipitation,¹⁰ electrolysis,¹¹ ion exchange,¹² membrane separation,¹³ and adsorption.¹⁴ As a final step for gold purification, electrowinning¹⁵, chemical reduction, or precipitation¹⁶ processes are used. Among these recovery methods, adsorption is one of the most widely used methods for gold recovery from e-wastewater due to its low cost, simple operation, and mild reaction conditions.¹⁷ However, traditional adsorbents like active carbon¹⁸ have shown limited selectivity for gold, which can be problematic due to the diverse and complex composition of e-wastewater that contains other

metal ions, including copper, iron, tin, nickel, lead, zinc, and silver.¹⁹ In recent years, researchers have developed many new functional materials, such as Zr-MOF,²⁰ chitosan,²¹ aminated microspheres,²² etc. It is crucial to develop a selective extraction method for gold recovery due to the significant reduction in recovery efficiency caused by interference from co-existing ions. Additionally, the use of a highly acidic solution for e-waste digestion can pose challenges to the stability of adsorbents.²³ As a consequence, there is a need for adsorbents with selective adsorption for gold and high stability in acidic conditions.

Conjugated polyaniline compounds are composed of various functional groups and geometric porous structures,²⁴ making them ideal adsorbents for wastewater recycling. Poly-m-phenylenediamine (PmPD) nanoparticles have been previously investigated for removing pollutants from wastewater, including Cr(VI), Ag(I), Pb(II), Hg(II), dyes, and anions.^{25, 26} In the context of gold recovery from e-wastewater, PmPD is considered promising as an adsorbent due to several attributes: the PmPD nanoparticles are positively charged in wide pH ranges, which attract metal ions that exist as anions (e.g., AsO_4^{3-} , AuCl_4^-) in aqueous solutions,^{27, 28} PmPD contains abundant amino groups that could provide strong coordination and suitable redox sites for gold ions in the wastewater; and PmPD nanoparticles are highly stable in extremely acidic solutions, making them suitable for long-term applications in e-wastewater. Overall, PmPD nanoparticles are expected to effectively recover precious gold in e-wastewater, which has not been examined in previous studies. Besides, PmPD is an ideal membrane material, demonstrating great potential in membrane separation due to its high-water permeability and excellent rejection performance. For example, a nanofiltration membrane based on PmPD was successfully exploited for lithium separation from hypersaline brines.²⁹ Thus, the selective adsorption of PmPD for gold, coupled with its membrane characteristics, allows for efficient gold recovery from e-wastewater

while also addressing the limitations of powder-based materials in recycling applications.

This paper presented a facile method for synthesizing gram-scale PmPD nanoparticles through copper-ion-assisted polymerization and the nanoparticles were utilized for gold recovery from e-wastewater. The recovery capacity and selective gold capture performance of PmPD nanoparticles were thoroughly investigated, and the mechanism of selective gold recovery was revealed through various characterization methods. Furthermore, a PmPD adsorptive membrane was fabricated and tested for its gold recovery potential from acidic e-wastewater, and its performance was evaluated using real e-wastewater to assess its potential in practical applications. Finally, the recovered Au on the PmPD membrane was used to treat phenol-containing water to realize the catalytic degradation of 4-nitrophenol. This study provides an effective and economical approach for recovering precious metal ions from e-wastewater.

Materials and Methods

Chemicals and Materials.

Analytical grade reagents were used without further purification in this work, and ultrapure water from a Millipore system (Millipore, Billerica, MA) was utilized for the preparation of all solutions. M-Phenylenediamine (MPD, 99%, Aldrich), $\text{CuCl}_2 \cdot 2\text{H}_2\text{O}$ (Macklin, China), NaIO_4 (99.5%, Macklin, China), and glutaraldehyde (GA, 50% in water, Aladdin China) were used to prepare the PmPD nanoparticles and membranes. Chloroauric acid (HAuCl_4 , 48~50% for Au, Macklin), potassium hexachloroplatinate (K_2PtCl_6 , 98%, Macklin, China), and potassium hexachloropalladate (K_2PdCl_6 , 26.2% for Pd, Macklin, China) were used in the adsorption and recovery tests. In addition, 4-nitrophenol ($\text{C}_6\text{H}_5\text{NO}_3$, 98%, Aladdin China) and sodium borohydride (NaBH_4 , 98%, Aladdin, China) were used to evaluate the catalytic activities of as-

recovered Au nanoparticles.

Synthesis of PmPD Nanoparticle and Membrane Preparation.

PmPD was synthesized in large quantities according to a modified procedure reported in previous works^{29,30}. As illustrated in Figure 1a, an MPD solution with an initial concentration of 25 g/L was mixed with a CuCl₂ solution at a final concentration of 15.75 g/L to form the PmPD complex. To accelerate the polymerization, 100 g/L NaIO₄ solution was added to the mixture and shaken on a reactor for 2 h at 150 rpm. The resulting PmPD nanoparticles were purified by filtering them through a nanofiltration membrane with a nominal pore size of 200 nm to remove the excess oxidant, and then redispersed into ultrapure water using an ultrasonic water bath (SB25-12DTD, Ningbo Xinzhi Biotechnology Co., Ltd., China). This process was repeated three times, and the purified PmPD nanoparticles were finally freeze-dried for future experiments. The PmPD adsorptive membranes was fabricated by adding 4 wt % of glutaraldehyde (GA) solution to the PmPD suspension, which was then cross-linked at 60 °C for 30 min. The cross-linked PmPD solution was filtrated using a nylon membrane (JIN TENG) in a Millipore device (UFSC40001 Stirred Cell) at 0.2 bar nitrogen compression to complete fabrication of the adsorptive membranes. The membrane was washed with ulttapure water until the flux was stable and then used for gold recovery.

Characterizations

The morphology and element distribution of the PmPD nanoparticles were characterized using scanning electron microscopy (SEM; Merlin, ZEISS, MA, U.S.A.) and transmission electron microscope (TEM; Talos F200X, FEI, MA, U.S.A.) coupled with energy-dispersive spectroscopy (EDS). The specific surface area and pore size of the PmPD nanoparticles were measured using a Brunner-Emmet-Teller (BET) analyzer (ASAP 2020, Micromeritics, USA). Raman spectroscopy

were performed on a LabRAM HR Evolution (HORIBA, Kyoto, Japan). X-ray diffraction (XRD; Rigaku Smartlab 9KW, Tokyo, Japan) and X-ray photoelectron spectroscopy (XPS, PHI 5000 Versaprobe III, ULVAC-PHI, Japan) were employed to identify the chemical compositions of PmPD nanoparticles and to explore the interaction mechanisms of the PmPD nanoparticles with gold species. The hydrodynamic size and zeta potentials of the synthesized PmPD particles under various conditions were obtained using a Zetasizer Nano ZS instrument (NanoBrook Omini, Brookhaven, NY, U.S.A.).

Gold Recovery by Suspended PmPD Nanoparticles

To investigate the Au adsorption kinetics at different pH by suspended PmPD nanoparticles, 3 mg of PmPD particles were suspended in 10 mL of chloroauric acid solution with an initial Au(III) concentration of 40 mg/L at room temperature, and the solution pH (2-6) was regulated by acetic acid buffer and NaOH. The sample was collected at fixed time intervals, and the remaining gold ion concentration in the filtrate was determined using inductively coupled plasma-optical emission spectroscopy (ICP-OES, iCAP 7000 SERIES, Thermo Fisher Scientific, U.S.A.) after filtration using a 0.22 μm nylon filter membrane to remove suspended PmPD particles. To study the adsorption isotherm, 10 mL of chloroauric acid solutions with initial Au(III) concentrations of 10, 50, 100, 200, 300, 500, 600, 800, and 900 mg/L were prepared separately and mixed with 3 mg of PmPD nanoparticles, followed by magnetic stirring at room temperature for 24 h. The equilibrium Au(III) adsorption density of the PmPD particles was calculated using Eq 1:

$$q_e = \frac{C_i - C_e}{m} \times V \quad (1)$$

where q_e is the adsorption density of Au by the PmPD (mg/g), C_i and C_e are the initial and equilibrium Au concentrations (mg/L), respectively, V refers to the volume of the solution (L), and m is the mass of the adsorbent (g).

To evaluate the selectivity of PmPD particles for gold in complex media, we investigated the impact of common anions (e.g., SO_4^{2-} , NO_3^- , Cl^- , H_2PO_4^-) and competing metal cations (e.g., Ni^{2+} , Zn^{2+} , Cd^{2+} , Hg^{2+} , Pb^{2+} , Fe^{3+} , Al^{3+}) on Au(III) uptake. Specifically, 3 mg of PmPD particles were suspended in 10 mL of chloroauric acid solution with an Au concentration of 50 mg/L and other competing ions at 50 mg/L. After a 24-h adsorption period, the adsorption equilibrium of all ionic species was ensured, and the selectivity of the PmPD particles to each ion species was evaluated using Eq 2:

$$K_d = V(C_0 - C_e)/(C_e \times m) \quad (2)$$

where K_d represents the distribution coefficient that describes the affinity of the adsorbent towards a particular ion (L/mg).

Gold Recovery by PmPD Membrane

The gold recovery by PmPD-base membrane was evaluated using a dead-end Millipore filtration system with a total internal volume of 50 mL and an active surface area of 12.56 cm². The chamber was filled with an aqueous solution containing Au(III) at a concentration of 40 mg/L, which was continuously supplied from a stock solution in a plastic container. Breakthrough curves under different materials loading (5, 10, 15, and 20 mg) and device flow rate (1, 2.5, 5, and 10 mL/min) were explored. Ten milliliter samples of the filtrate were periodically collected and analyzed by ICP-OES. To determine the regeneration performance of the PmPD adsorptive membrane, a 1:1 (v/v) solution of thiourea (1 mol/L) and HCl (1 mol/L) was passed through the membrane containing the adsorbed Au for 60 min in the single-pass mode. The filter was then rinsed with copious ultrapure water until the effluent pH reached neutral, and a new adsorption cycle was initiated using a solution of Au(III) at the same concentration of 40 mg/L and a flow rate of 2.5 mL/min.

A case study was performed on Au recovery from actual electronic wastewater. The printed circuit board (15 cm×10 cm) was digested by 300 mL aqua fortis solution and the concentration of gold and other metal ions (Zn^{2+} , Pb^{2+} , Cu^{2+} , Fe^{3+} and Al^{3+}) in the e-wastewater was measured by ICP-OES. The actual e-wastewater was passed through the Millipore cell containing PmPD membrane (15 mg) at a flow rate of 2.5 mL/min. The filtrate was collected on the other side of the container and diluted to test the concentration of Au and other metal ions by ICP-OES. The recovery efficiency of gold and other metal ions in e-wastewater were obtained.

Catalytic Performance by Au@PmPD Membrane

The catalytic activity of the recovered Au on the PmPD membrane (referred as Au@PmPD) was evaluated by photometrically monitoring the reduction of 4-NP to 4-aminophenol (4-AP). Firstly, the Au@PmPD membranes were prepared using the experiments described earlier, where the $H AuCl_4$ solution passed through the PmPD membranes (15 mg), and the gold (4 mg) was immobilized onto the membranes. Subsequently, a feed solution containing 20 mg/L 4-NP and 0.025 M $NaBH_4$ was passed through a Millipore device containing the Au@PmPD membrane. After the catalytic reduction reaction, the resulting product 4-AP was monitored by a UV–vis spectrometer at 300 nm (Figure S1). The catalytic processes were performed under pressures ranging from 0.2 to 2.6 bar. The apparent rate constant of reduction (K_{ops}) was calculated using Eq 3.

$$\ln(C_t / C_0) = -k_{ops}t \quad (3)$$

where C_t and C_0 are the concentrations of the 4-NP at time t and 0, respectively.

To further evaluate the superiority of the catalysis, apparent rates of dynamic and static catalysis were calculated. The apparent rates could be considered constant under the catalysis

process as the concentration of NaBH₄ was higher than that of 4-NP. Thus, the apparent rate constants could be calculated by the following Eq 4:³¹

$$\ln \frac{C_t}{C_0} = -k_{app}t \quad (4)$$

where C_t and C_0 are the concentration at reaction time t and the initial concentration of 4-NP, respectively, and k_{app} is the apparent rate constant (min^{-1}).

Results and Discussion

Characterization of PmPD nanoparticles. PmPD nanoparticles were prepared using a modified oxidative polymerization method, with the MPD monomer serving as the ligand, Cu²⁺ as the complex metal, and NaIO₄ as the oxidation agent (Figure 1a). The SEM and TEM images in Fig 1b and 1c, respectively, reveal that the PmPD nanoparticles aggregated, with the individual particles in size at tens of nanometers. The PmPD nanoparticles have a specific surface area of 75.49 m²/g and a pore volume of 0.37 cm³/g (Figure 1d), which is comparable to some traditional materials (e.g., chitosan) but much lower than that of the porous material (e.g., Zr-MOF). Moreover, the structure of PmPD was analyzed with Raman spectroscopy (Figure 1e). The G- and D-band (~ 1573 and ~ 1352 cm⁻¹) implies the presences of the benzenoid and quinoid bonds of the PmPD, respectively.³²

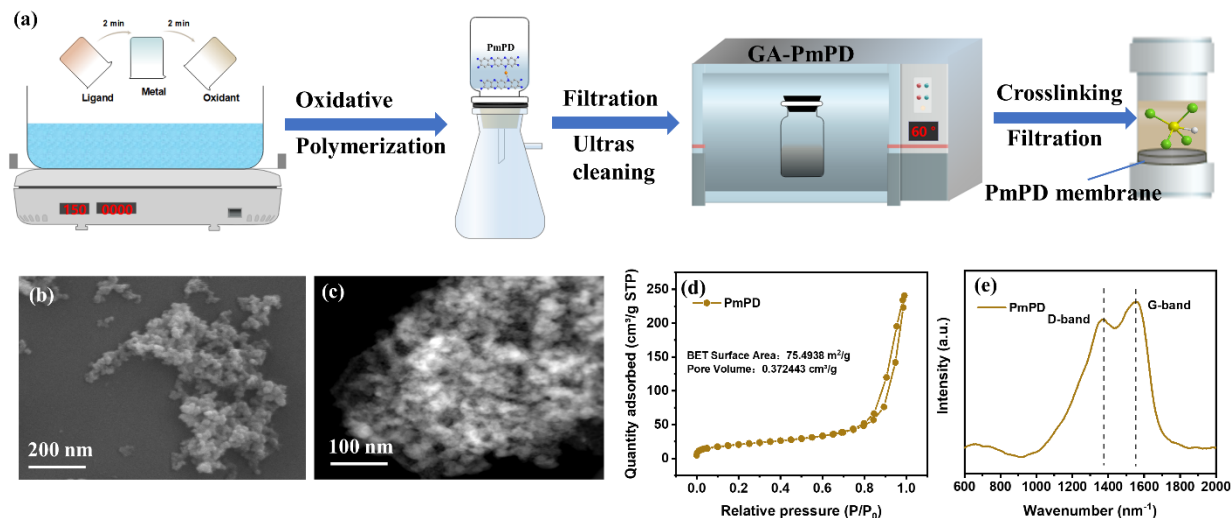


Figure 1. Preparation and characterization of the PmPD particles and membranes: (a) fabrication route of PmPD; (b) SEM image and (c) TEM image of PmPD particles; (d) N₂ adsorption-desorption isotherm; and (e) the Raman spectra of PmPD.

Adsorption performance of Gold by PmPD Nanoparticles. Figure 2a shows the adsorption kinetics of Au by PmPD nanoparticles at different pH conditions. The results show that the adsorption rate of Au(III) by PmPD nanoparticles was rapid, with the initial concentration of 40 mg/L decreasing to zero within 1 min. We note that complete removal were achieved even in acidic condition (pH 2), implying that the PmPD material would have a good application in the acid leaching solution. At higher concentration of Au(III) (160 mg/L), the removal kinetics could be accurately described by the pseudo-second-order model ($R^2 = 0.99$, Figure S2), indicating that the chemisorption process was the rate-limiting step.

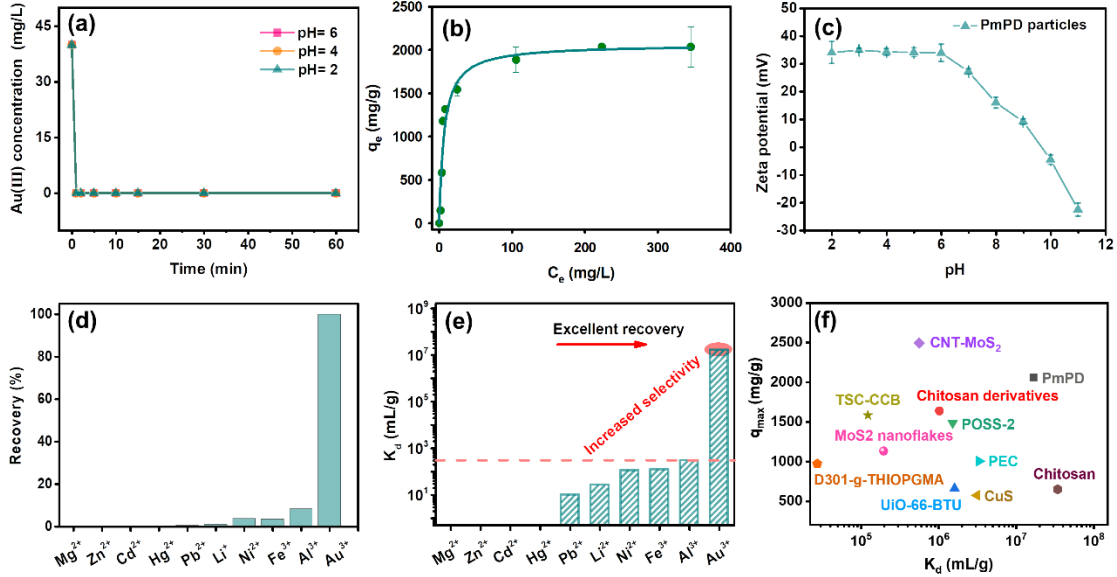


Figure 2. Adsorption characteristics of PmPD particles for Au(III) removal ($[Au(III)]_0 = 40$ mg/L): (a) the effect of pH on the Au adsorption rate; (b) isotherm of Au(III) adsorption by PmPD particles fitted by Langmuir model (solid line); (c) zeta potential measurements of PmPD at pH ranging from 2 to 11; (d) removal of various cations by PmPD particles in a mixture containing different ions at equal concentration (50 mg/L); (e) distribution coefficients (K_d) of various cation species; (f) comparison of maximum adsorption capacities (q_{max}) and distribution coefficient (K_d) of PmPD particles with those of other reported adsorbents in the literature.³³⁻³⁹

Figure 2b shows the adsorption isotherms of Au(III) by the PmPD nanoparticle suspension at room temperature. At the tested conditions, Au adsorption density q_e increased rapidly with further increasing Au equilibrium concentration C_e and eventually reached a constant value. The adsorption isotherm data in Figure 2b was well-fitted by the Langmuir adsorption model with a high correlation coefficient ($R^2 = 0.99$, Figure S3), indicating a monolayer sorption of Au(III) onto the PmPD nanoparticle surface.³⁴ The maximal adsorption capacity of Au(III) ions on the PmPD nanoparticles was determined to be ~ 2063 mg/g. Compared to other materials (e.g., Zr-MOF), the PmPD nanoparticles displayed a large adsorption capacity for gold despite smaller specific surface area. The excellent adsorption for gold could be partly attributed to the electrostatic attraction of positively-charged PmPD nanoparticles at pH values below 6 (Figure 2c) and the negatively charged $AuCl_3(OH)^-$ or $AuCl_2(OH)_2^-$ complexes formed in aqua regia leaching solutions.⁴⁰

However, the ultrafast adsorption and high capacity suggested the possible existence of other interaction between Au ions and PmPD nanoparticles, which require further exploration. Considering the strong acidic environment in the e-waste etching solution, we conducted the rest of the tests at pH 2, unless otherwise noted.

Selectivity of PmPD Particles towards Different Ions. To investigate the selectivity of PmPD particles towards different cations, we evaluated their adsorption capabilities several co-existing metal cations (Li^+ , Ni^{2+} , Zn^{2+} , Cd^{2+} , Hg^{2+} , Pb^{2+} , and Fe^{3+}) present in e-waste etching solution as well as some common cations (Mg^{2+} and Al^{3+}). The adsorption experiment was carried out in a mixed solution containing Au(III) and other cations at a concentration of 50 mg/L. As shown in Figure 2d, PmPD particles exhibit a separation efficiency of up to 100% for Au(III) within 1 hour. For other cations, however, PmPD particles either did not exhibit any removal (Mg^{2+} , Zn^{2+} , Cd^{2+} , Hg^{2+} , Pb^{2+} and Li^+) or very low removal efficiency ($< 15\%$ for Fe^{3+} , Ni^{2+} , and Al^{3+}). The reason was metal complex formation: the amine groups in PmPD have the potential to form complexes with metal ions, so Fe^{3+} , Ni^{2+} , and Al^{3+} ions that could form relatively stronger complexes with the amine groups were adsorbed to some extent. Given the high concentrations of Cu in the acidic etching solutions of e-waste,⁴¹ we also investigated the ability of PmPD particles to remove Au in the presence of various concentrations of Cu, up to 5000 mg/L, which is 100 times higher than that of Au ions. The results, as shown in Figure S4, indicated that PmPD particles completely removed Au ions, while the separation efficiency of Cu was less than 1% across all ratios, even at the highest Cu concentrations.

To reveal the degree of affinity of the PmPD nanoparticles to different cations, we calculated distribution coefficients (K_d , mL/g) for each species using Eq 2. In general, a K_d value of 10^4 mL/g is an indicator of high selectivity of an adsorbent to the target.⁴² The PmPD nanoparticles exhibited

an adsorption affinity with a decreasing order of $\text{Au}^{3+} \gg \text{Al}^{3+} > \text{Fe}^{3+} > \text{Ni}^{2+} > \text{Li}^+ > \text{Pb}^{2+} > \text{Hg}^{2+} > \text{Cd}^{2+} > \text{Zn}^{2+} > \text{Mg}^{2+}$ (Figure 2e). Specifically, K_d value of the PmPD nanoparticles for Au(III) reached as large as 1.67×10^7 mL/g, almost 2-3 orders of magnitude higher than that of any other metallic cations tested in this study. The gold removal performance of the PmPD nanoparticles was compared with other materials reported regarding to their respective capacity, affinity and acidic level (Table S1). As shown in Figure 2f, the PmPD nanoparticles exhibited a high gold adsorption capacity (2063.09 mg/g) and an extremely high affinity K_d (1.67×10^7 mL/g), outperforming most materials previously reported, including POSS-2,³⁹ PEC,³⁶ and CuS³⁸ nanoparticles. The exceptional selectivity of PmPD nanoparticles to gold can be attributed to the anion existing species of gold, which is different from other competing metals that mainly exist in cationic form. These cations exhibit electrostatic repulsion to the protonated PmPD nanoparticles under acidic conditions. Moreover, previous studies have demonstrated that the binding energies of the gold with amino groups are relatively high (53.0 kJ/mol),⁴³ and the N species in the PmPD nanoparticles can readily form a complex with gold. The addition of different anions such as Cl^- , H_2PO_4^- , NO_3^- , or SO_4^{2-} did not affect the complete removal of gold within 1 min by PmPD nanoparticles (Figure S5). Therefore, gold is completely adsorbed within 1 min even in the interference of anions, and PmPD still maintained a good selective adsorption performance for gold over a long period of time. Collectively, these findings clearly demonstrated the outstanding selectivity and high capacity of PmPD nanoparticles for capturing Au(III) and their ability to overcome the interference from the co-existing ions in the e-wastewater.

Mechanism of Gold Recovery by PmPD. To gain a deeper understanding of the gold recovery mechanisms by PmPD nanoparticles, we conducted multiple characterization techniques to

analyze the structure of both fresh and Au-loaded PmPD particles. SEM analysis (Figure S6) revealed that fine particles were formed and attached onto the surface of the PmPD nanoparticles following the adsorption of Au(III). Furthermore, the newly formed nanoparticles were also observed through the TEM imaging (Figure 3a), and their metallic gold nature was confirmed by EDS mapping analysis. XRD analysis showed that there were no diffraction peaks in the pristine PmPD sample, indicating the amorphous nature of the as-prepared polymeric particles. However, after gold capture, diffraction peaks at 38.2° (111), 44.6° (200), 64.7° (220), 77.6° (311) were observed, which were assigned to characteristic planes of metallic gold. Collectively, these characterizations imply that a reduction of Au(III) to metallic gold nanoparticles occurred during the recovery process in addition to Au(III) adsorption.

To explicitly elucidate the chemical sites involved in the reaction, XPS was used to characterize the PmPD particles before and after gold recovery. The Au 4f XPS spectra of the Au-loaded sample showed the presence of mixed Au components (Figure 3c). Deconvolution analysis revealed the peaks at binding energies of 83.7 and 87.4 eV, which were attributed to Au 4f_{7/2} and Au 4f_{5/2} of Au(0), respectively, while the peaks at 85.1 and 88.7 eV were attributed to Au 4f_{7/2} and Au 4f_{5/2} of Au(I), respectively. The co-existence of Au(0) and Au(I) in the XPS spectra confirmed the reductive recovery of Au(III) ions from water by the formation of metallic Au nanoparticles and intermediate Au(I) on PmPD. The N 1s spectra (Figure 3d) showed the peaks at 398.8, 399.6, 400.9, and 401.9 eV associated with -NH- in the benzenoid amine units, -N=C- in both quinoid imine and phenazine, -N-C- and $\text{-N}^+=$ of PmPD, respectively. Comparing the N 1s spectra before and after gold adsorption, the overall peak shifted towards a higher binding energy after gold recovery. Specifically, the deconvolution analysis showed that the content of -NH- groups decreased from 62.3% to 18.4%, while that of -N=C- groups increased from 19.2% to

58.9%. Meanwhile, in the C 1s XPS spectra (Figure 3e), the peak at 285.9 eV representing -C=N- significantly increased from 24.7% to 33.1%, while the peak at 287.42 eV associated with the C–N group substantially declined after the Au ion recovery. These results suggested that, along with the adsorption and reduction of Au(III), the -NH- of conjugated polymers was readily oxidized by Au(III) and finally transformed to -N=C- group.

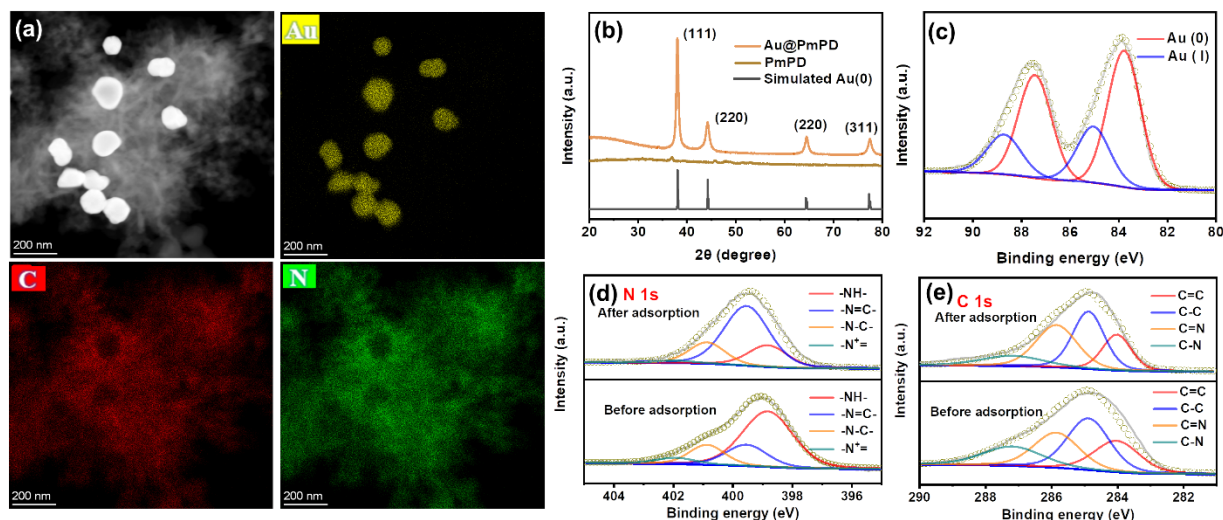


Figure 3. Au(III) recovery by PmPD characterized by various tools: (a) TEM and elemental mapping of the PmPD nanoparticles after Au(III) recovery; (b) XRD patterns before and after Au(III) recovery and metallic Au reference (PDF 04-0784); (c) high-resolution Au 4f XPS spectra after Au(III) recovery; (d, e) deconvolution analysis of N 1s and C 1s XPS spectra of PmPD before and after Au recovery.

Additional *in-situ* XRD and *in-situ* FTIR were performed to further understand the temporal compositional change of gold and PmPD. To ensure the complete recovery of gold from the solution within 10 min, an overdosed PmPD was used. As shown in Figure 4a, the XRD peaks of metallic gold were barely visible at 10-min mark but gradually strengthened with increasing reaction time. This suggests a two-step adsorption-redox process of gold capture: Au(III) ions were rapidly adsorbed by the PmPD particles within the first 10 min and gradually reduced on the adsorbent over time. *In-situ* FT-IR absorption spectra of PmPD (Figure 4b) showed the two peaks

at $\sim 1620\text{ cm}^{-1}$ and $\sim 1500\text{ cm}^{-1}$, which can be attributed to the stretching vibrations of quinoid imine ($\text{C}=\text{N}$) and benzenoid amine structures ($\text{C}-\text{N}$), respectively. The relative intensity of these two peaks ($C_{(\text{C}-\text{N}/\text{C}=\text{N})}$) has important implications in the adsorption and reduction mechanisms of gold by the PmPD particles. At the start of experiments ($<10\text{ min}$), the value of $C_{(\text{C}-\text{N}/\text{C}=\text{N})}$ barely changed, suggesting the adsorption was the dominant separation process during this period. However, the decrease in $C_{(\text{C}-\text{N}/\text{C}=\text{N})}$ became much more pronounced with increasing $\text{C}=\text{N}$ peak and the weakening $\text{C}-\text{N}$ peak afterwards, in line with the reduction process as demonstrated by the N 1s XPS.

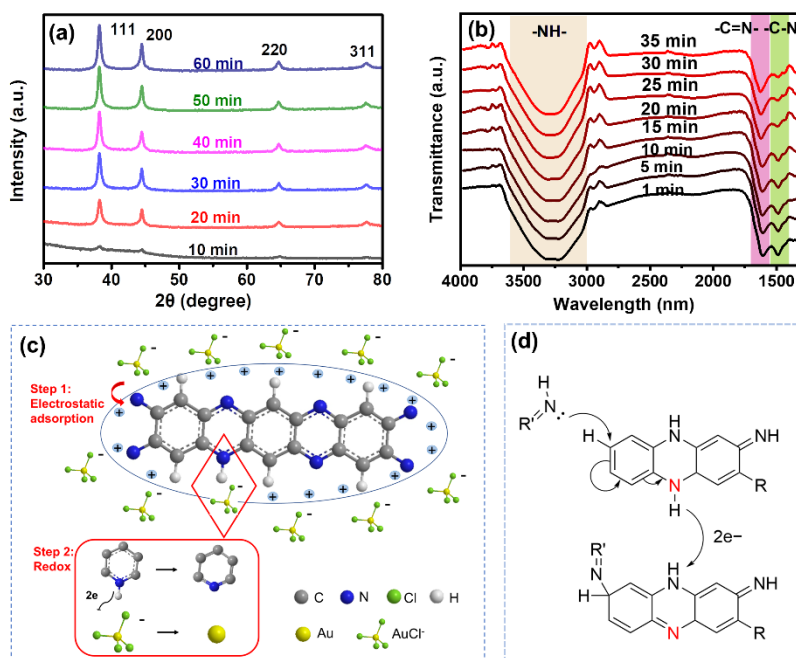


Figure 4. Adsorption-redox mechanisms of Au recovery by PmPD: (a) *in situ* time-resolved XRD patterns and (b) *in situ* time-resolved FT-IR spectra of Au-laden PmPD particles; (c, d) proposed mechanism of Au adsorption-reduction on the PmPD particles.

Collectively, the mechanisms of Au(III) recovery by PmPD nanoparticles can be summarized and illustrated in Figure 4c and Figure 4d. Initially, anionic AuCl_4^- were attracted to the positively charged surface of the PmPD nanoparticles *via* electrostatic forces, contributing to the fast removal

kinetics at a range of pH conditions. The N sites in the PmPD nanoparticles exhibit a high affinity as the adsorption sites for Au ions via complexation, which enables the excellent selectivity of PmPD particles to gold and good anti-interference capability to the co-existing ions. The adsorbed Au(III) was then reduced to Au(0) in a series of steps, with Au(I) as the primary intermediate. Meanwhile, the C–N group in the PmPD was oxidized to a C=N group. Finally, the resulting metallic gold nanoparticles attached to the surface of PmPD particles. Overall, the combination of electrostatic attraction, complexation, and reduction processes make PmPD nanoparticles an effective agent for the recovery of Au(III) ions from water.

Recovery of Gold by PmPD Adsorptive Membrane. Based on the excellent separation efficiency for gold and our understanding on the underlying mechanisms, we developed an adsorptive membrane using the PmPD particles as building blocks (Figure 5a). The resulting PmPD membrane was highly stable in solution without the release or resuspension of PmPD particles, thanks to the GA crosslinking. The SEM image (Figure S7) showed that the PmPD particles were evenly distributed on the substrate, and the overall PmPD membrane exhibited a porous structure with substantial channels and surface area for water filtration and anchoring of the gold.

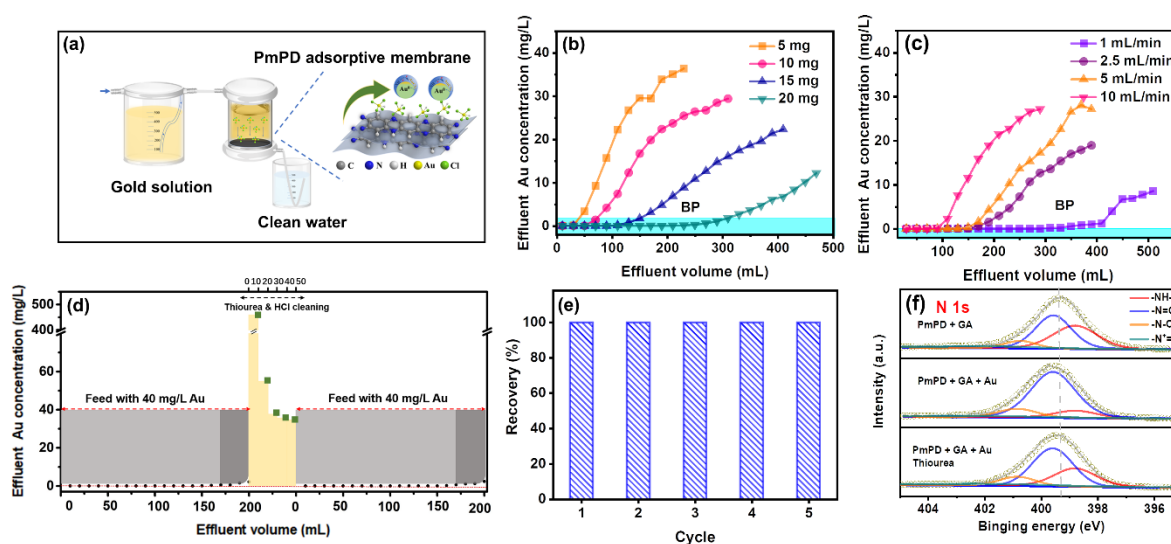


Figure 5. Performance of PmPD adsorptive membrane for Au recovery: (a) the schematic representation of the membrane-based Au recovery process; (b) the effects of PmPD membrane mass (flow rate = 2.5 mL/min) and (c) flow rate on the recovery of gold (the mass of PmPD = 15 mg); (d) the regeneration of PmPD membrane using 1 mol/L thiourea and 1 mol/L HCl cleaning for a new cycle of Au recovery; (e) the regeneration efficiency of membrane-based Au(III) recovery ($[\text{Au(III)}]_0 = 40 \text{ mg/L}$, $\text{pH} = 2.5$, flow rate = 2.5 mL/min); and (f) high-resolution N 1s XPS spectra after Au(III) recovery and after the regeneration of the PmPD membrane.

After passing through the adsorptive membrane, the concentration of Au(III) in the feed solution was significantly reduced from 40 mg/L to a few micrograms per liter in the effluent (Figure 5b), demonstrating that the PmPD membranes could effectively recover gold from solution in the single-pass filtration mode. The treatment capacity of the adsorptive membrane was determined by the total effluent volume at the breakthrough point (when Au emerges in the effluent), and was found to be dependent on the PmPD mass in the membrane as well as the operating flow rate. Increasing the mass of PmPD from 5 to 10, 15 and 20 mg, resulted in an increase in the treatment capacity from ~50 to ~100, ~150, and ~300 mL, respectively (Figure 5b). Consequently, the average effective gold separation capacity using the PmPD adsorptive membranes was determined to be ~530 mg/g. We note that the effective removal capacity of the membrane was substantially smaller than that obtained using suspended PmPD particles in the batch study. This difference is ascribed to the shorter contact time between the PmPD membrane and gold (< 3 s, Text S1), compared to the longer contact time in batch tests lasting for several hours under the non-equilibrium conditions. Figure 5c shows that the treatment capacity was increased by over three times when the flow rate decreased from 10 to 1 mL/min, suggesting that the recovery performance can be substantially enhanced by optimizing the operation conditions including the membrane thickness and operating flow rate. Overall, despite of the limited interaction time, PmPD membranes exhibited excellent separation efficiency for gold recovery.

The regeneration and reuse of the PmPD membrane were evaluated to determine its practical feasibility. Thiourea/HCl solution was used to recover the membrane, followed by supplying new

gold feed solutions. As shown in Figure 5d, the PmPD membrane collected about 6.8 mg of gold in the first filtration cycle before the breakthrough, and flushing it with 50 mL thiourea/HCl solution was able to recover ~ 6.25 mg of gold from the membrane. It is noteworthy that the concentration of enriched gold in the first 10 mL of thiourea/HCl solution was as high as 460 mg/L, more than 11 times higher than the Au concentration in the feed solution, confirming that the gold enriched on the PmPD adsorptive membrane can be extracted and is more valuable for practical applications. Thiourea can form stable $\text{Au}[\text{SC}(\text{NH}_2)_2]^{2+}$ complex cation with gold,⁴⁴ which is desorbed from the adsorptive membrane. Simultaneously, PmPD membranes were reduced with N–C and N=C of PmPD restoring to the original content as evidenced by the N 1s XPS spectra (Figure 5f). After regeneration, the recovered PmPD membrane could achieve the same mass for recovering gold in the second filtration cycle (Figure 5d). This suggests that the PmPD membrane can be entirely restored to achieve the same adsorption performance as the previous cycle. In addition, the recovery efficiency of 100% could be maintained for at least five consecutive cycles (Figure 5e), illustrating that PmPD membrane possess excellent regenerative properties. These findings demonstrated the practical feasibility of PmPD membranes for gold recovery and its potential for commercial applications.

Practical application of a PmPD adsorptive membrane. The PmPD adsorptive membrane's practical application was tested for the recovery of gold from acidic aqua regia, which is commonly used to leach gold from circuit boards in practical applications and resulting in an extremely acidic gold-containing leachate. The solution contained 4776 mg/L of Zn^{2+} , 57 mg/L of Pb^{2+} , 33133 mg/L of Cu^{2+} , 11908 mg/L of Fe^{3+} , 1618 mg/L of Ni^{2+} , 2100 mg/L of Al^{3+} and 7.6 mg/L Au^{3+} (Figure 6a). To confirm the excellent performance of PmPD membrane on Au recovery, a typical experiment was conducted using a membrane fabricated with 15 mg PmPD to recover 10 mL of

acidic leachate. The recovery efficiencies of different metals by PmPD membrane were presented in Figure 6b, exhibiting 0%, 0.23%, 1.08%, 6.71%, 8.22% and 100% for Cu^{2+} , Fe^{3+} , Al^{3+} , Ni^{2+} , Zn^{2+} and Au^{3+} , respectively. The PmPD membrane achieved complete recovery of gold, even in the presence of other competing cations and a large number of anions (Cl^- , NO_3^-) at much higher concentrations. This result demonstrates that the PmPD membrane maintained excellent adsorption selectivity in recovering Au (III) from practical acidic leachates. Due to the coexistence of other metals like Zn, further treatments may be required for purification. For example, thiourea could be used for the re-dissolution of Au from the PmPD membrane.⁴⁴ Following the aforementioned treatment, an Au solution with a significantly higher concentration can be obtained, which underscores the economic advantages of our treatment approach compared to direct gold sedimentation from the wastewater in a much larger volume.

Numerous studies have shown successful attempts to use gold nanoparticles as efficient catalysts.⁴⁵⁻⁴⁷ To prove the applicability of as-collected Au(0) on the membrane, a typical catalytic degradation of 4-NP to 4-AP was tested evaluating the catalytic performance of the Au@PmPD membrane. As shown in Figure 6c, the characteristic absorbance of 4-NP at 400 nm gradually decreased at a flow rate of 2.5 mL/min. Correspondingly, the characteristic absorbance of 4-AP at 300 nm increased. Figure 6d demonstrated that the 4-NP concentration $\ln(C_t/C_0)$ was linearly correlated to the reaction time ($R^2 = 0.92$). The reaction kinetics constant of the Au@PmPD membrane was 0.59 min^{-1} in reducing 4-NP, which was faster than the 0.24 min^{-1} obtained from the dispersion of PmPD after Au uptake (Figure S8). The results indicated that the *in-situ* immobilization of gold nanoparticles on the surface of PmPD membrane possessed a faster catalytic reduction. This is because of the enhanced transport and diffusion of 4-NP and NaBH_4 onto catalytic Au sites enabled by the membrane filtration. Overall, the results suggested a

potential application of Au@PmPD on creating catalytic membrane microreactors, which allows the "waste" to be transformed into treasure.

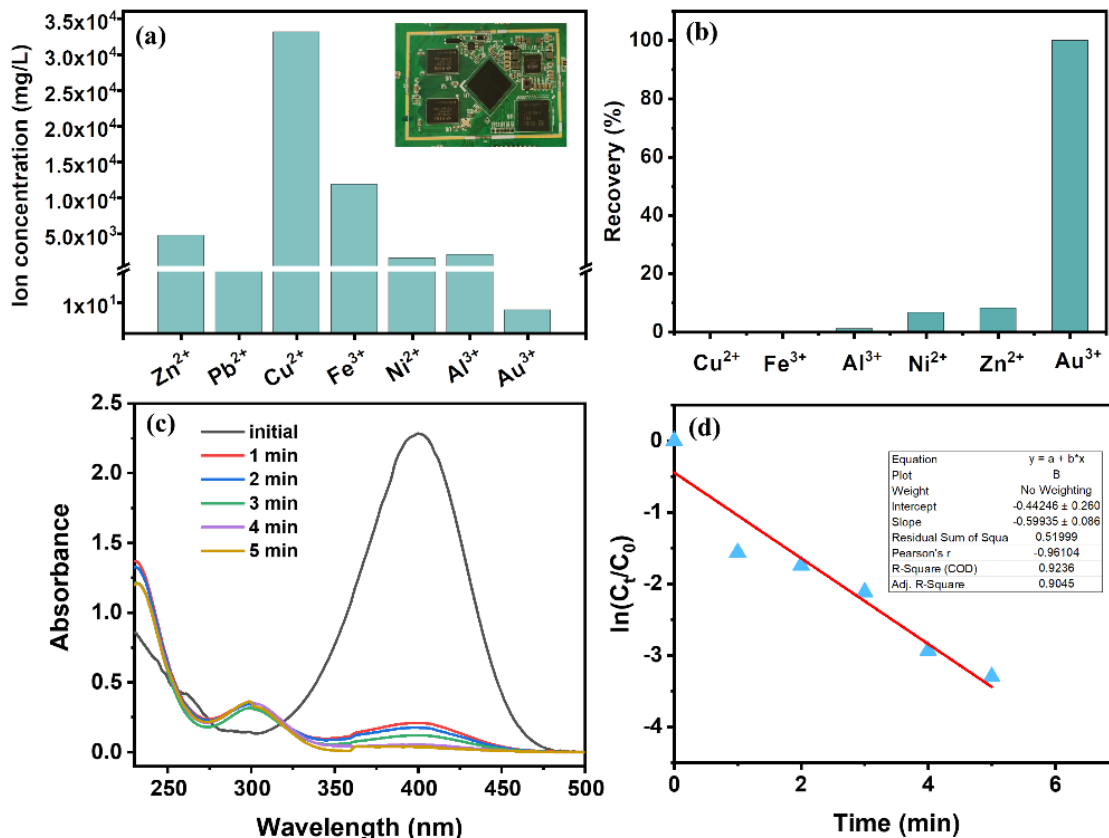


Figure 6. Application of PmPD in actual e-wastewater: (a) the concentration of metal ions in the leachate of the circuit board (with the image of the circuit board in the picture), (b) recovery of various cations by PmPD membrane in e-wastewater, (c) UV-vis spectra of 4-NP solution in the flow-through system; and (d) apparent pseudo-first-order rate constant as slope of the linear fit $\ln(C_t/C_0)$ over time. The $NaBH_4$ was added in a concentration of 25 mM.

Conclusions

In conclusion, this study presents a novel and efficient approach for recovering gold from e-wastewater using PmPD nanoparticles and an adsorptive membrane. The coordination interaction between gold and amino functional groups on PmPD nanoparticles enables selective recovery of gold from complex mixtures of heavy metals, addressing the challenges of selective gold recovery

from e-waste. The PmPD adsorptive membrane provides a simple and effective method for gold recovery from e-wastewater under extremely acidic conditions, offering a practical solution for e-waste treatment. Furthermore, the Au@PmPD membrane can be recycled to degrade *p*-nitrophenol, demonstrating its potential for use as a catalytic membrane microreactor. Overall, this technology provides a sustainable and environmentally friendly approach to gold recovery, with the potential to improve recovery efficiency and decrease secondary waste. The findings of this study have implications for the development of resource recovery and reuse technologies, contributing to the sustainable management of e-waste and the transition towards a circular economy.

Associated Content

Supporting Information

Additional results are available in the Supporting Information, including the recovery of Au(III) at different ratios of copper and Au, SEM images of PmPD after Au(III) adsorption, EDS elements distribution of Au, C, N after Au(III) adsorption, *etc.* This material is available free of charge *via* the Internet at <http://pubs.acs.org>.

Acknowledgements

This project was financially supported by the Stable Support Plan Program of Shenzhen Natural Science Fund (Grant No. 20200925155303001), SUSTech-MIT Joint Center for Mechanical Engineering Education and Research, and State Environmental Protection Key Laboratory of Integrated Surface Water-Groundwater Pollution Control. The authors acknowledge the assistance of SUSTech Core Research Facilities.

Reference

- (1) Kim, H. J.; Lee, J. S.; Park, J. M.; Lee, S.; Hong, S. J.; Park, J. S.; Park, K. H. Fabrication of Nanocomposites Complexed with Gold Nanoparticles on Polyaniline and Application to Their Nerve Regeneration. *ACS Appl Mater Interfaces* **2020**, *12* (27), 30750–30760.
- (2) Zhang, K.; Sharma S. Site-Selective, Low-Loading, Au Nanoparticle–Polyaniline Hybrid Coatings with Enhanced Corrosion Resistance and Conductivity for Fuel Cells. *ACS Sustainable Chem. Eng.* **2017**, *5*, 277–286.
- (3) Ding, Y.; Zhang, S.; Liu, B.; Zheng, H.; Chang, C.; Ekberg, C. Recovery of Precious Metals from Electronic Waste and Spent Catalysts: A Review. *Resour Conserv Recy* **2019**, *141*, 284–298.
- (4) Sheaffer, K. N. Mineral Commodity Summaries. Ksheaffer@usgs.gov. **2022**, 703, 648–4954.
- (5) Yang, S.; Li, T.; Cheng, Y.; Fan, W.; Wang, L.; Liu, Y.; Bian, L.; Zhou, C.; Zheng, L.; Cao, Q. Covalent Organic Framework Isomers for Photoenhanced Gold Recovery from E-Waste with High Efficiency and Selectivity. *ACS Sustainable Chem. Eng.* **2022**, *10*, 9719–9731.
- (6) Shahabuddin, M.; Nur Uddin, M.; Chowdhury, J. I.; Ahmed, S. F.; Uddin, M. N.; Mofijur, M.; Uddin, M. A. A review of the recent development, challenges, and opportunities of electronic waste (e-waste). *Int J environ Sci Te* **2023**, *20*, 4513–4520.
- (7) Duan, H.; Zhu, X. N. Recent Advances in Recovering Technology for Recycling Gold from Waste Printed Circuit Boards: A Review. *Energy Sources, Part A: Recovery, Utilization, and Environmental Effects.* **2022**, *44* (1), 1640–1659.
- (8) Sun, D. T.; Gasilova, N.; Yang, S.; Oveisi, E.; Queen, W. L. Rapid, Selective Extraction of Trace Amounts of Gold from Complex Water Mixtures with a Metal-Organic Framework (MOF)/Polymer Composite. *J Am Chem Soc.* **2018**, *140* (48), 16697-16703.
- (9) Bui, T.; Lee, W.; Jeon, S-B.; Kim, K-W.; Lee, Y. Enhanced Gold(III) adsorption using glutaraldehyde-crosslinked chitosan beads: Effect of crosslinking degree on adsorption selectivity, capacity, and mechanism. *Sep Purif Technol* **2020**, *248*, 116989.
- (10) Juárez-López, G.; Landero, R.; Cardona, F. P.; Velazquez-Cruz, E. I.; Yescas-Mendoza, E.; Martínez-Martínez, R. The Sodium Dithionite Influence During Complex Precipitation of Au⁺-S₂O₃²⁻. *Gold Bull.* **2017**, *50* (1), 25–32.
- (11) Wang, H.; Wu, Y.; Deng, N.; Li, B.; Li, F.; He, J. B. Development of A Bipolar Electrochemical Flow Microreactor for Recovery of Valuable Metals from Mixed Solutions. *Chemical Engineering Journal.* **2020**, *382*, 121907.
- (12) Choi, J. W.; Song, M. H.; Bediako, J. K.; Yun, Y. S. Sequential Recovery of Gold and Copper from Bioleached Wastewater Using Ion Exchange Resins. *Environ Pollut.* **2020**, *266*, 115167.
- (13) Kubota, F.; Kono, R.; Yoshida, W.; Sharaf, M.; Kolev, S. D.; Goto, M. Recovery of Gold Ions from Discarded Mobile Phone Leachate by Solvent Extraction and Polymer Inclusion Membrane (PIM) Based Separation Using An Amic Acid Extractant. *Sep. Purif. Technol.* **2019**, *214*, 156–161.
- (14) Kim, K. R.; Choi, S.; Yavuz, C. T.; Nam Y. S. Direct Z-Scheme Tannin–TiO₂ Heterostructure for Photocatalytic Gold Ion Recovery from Electronic Waste. *ACS Sustainable Chemistry & Engineering.* **2020**, *8* (19), 7359–7370.
- (15) Murali, A.; Zhang, Z.; Shine, A.; Free, Michael.; Sarswat, Prashant. E-wastes derived sustainable Cu recovery using solvent extraction and electrowinning followed by thiosulfate-based gold and silver extraction. *J Hazard Mater* **2022**, *8*, 100196.

- (16) Ray, D.; Baniasadi, M.; Graves, J.; Greenwood, A.; Farnaud, S. Thiourea Leaching: An Update on a Sustainable Approach for Gold Recovery from E-waste. *J Sustain Metall* **2022**, *8*, 597–612.
- (17) Wang, C.; Lin, G.; Zhao, J.; Wang, S.; Zhang, L.; Xi, Y.; Li, X.; Ying, Y. Highly Selective Recovery of Au(III) from Wastewater by Thioctic Acid Modified Zr-MOF: Experiment and DFT Calculation. *Chem. Eng. J.* **2020**, *380*, 122511.
- (18) Xia, J.; Mahandra, H.; Ghahreman, A. Efficient Gold Recovery from Cyanide Solution Using Magnetic Activated Carbon. *ACS Appl. Mater. Interfaces* **2021**, *13* (40), 47642–47649.
- (19) Cyganowski, P.; Garbera, K.; Leśniewicz, A.; Wolska, J.; Pohl, P.; Jermakowicz D. The Recovery of Gold from The Aqua Regia Leachate of Electronic Parts Using A Core–Shell Type Anion Exchange Resin. *J. Saudi Chem. Soc.* **2017**, *21* (6), 741–750.
- (20) Chang, Z.; Li, F.; Qi, X.; Jiang, B.; Kou, J.; Sun, C. Selective and Efficient Adsorption of Au (III) in Aqueous Solution by Zr-Based Metal-Organic Frameworks (MOFs): An Unconventional Way for Gold Recycling. *J Hazard Mater.* **2020**, *391*, 122175.
- (21) Wu, J.; Wang, Y. Immobilized Chitosan as A Selective Absorbent for The Nickel Removal in Water Sample. *J Environ Sci.* **2003**, *15* (5), 633–638.
- (22) Zhao, L.; Hu, X.; Zi, F.; Chen, S.; Cheng, H.; Yang, P.; Zhang, Y.; Chen, Y.; Jiang, Y.; Li, X.; Lin, Y.; Li, Z.; Li, J.; Wang, H.; Li, Y. Development of Stable, Efficient, and Recyclable Amine-Containing Microspheres for Gold(I) Thiosulfate Complex Recovery. *ACS Sustain Chem Eng* **2022**, *10* (44), 14624–14635.
- (23) Iannicelli, E. M.; Giani, M. I.; Recanati, F.; Dotelli, G.; Puricelli, S.; Cristiani, C. Environmental Impacts of A Hydrometallurgical Process for Electronic Waste Treatment: A Life Cycle Assessment Case Study. *J Clean Prod.* **2017**, *140*, 1204–1216.
- (24) Hu, Y.; Tong, X.; Zhuo, H.; Zhong, L.; Peng, X. Biomass-Based Porous N-Self-Doped Carbon Framework/Polyaniline Composite with Outstanding Supercapacitance. *ACS Sustainable Chemistry & Engineering* **2017**, *5* (10), 8663–8674.
- (25) Steplin, S.; Kumar, Ganesh A.; Sarala, L.; Rajaram, R.; Sathiyam, A.; Merlin, J.; Lydia, I. Photocatalytic Degradation of Rhodamine B Using Zinc Oxide Activated Charcoal Polyaniline Nanocomposite and Its Survival Assessment Using Aquatic Animal Model. *ACS Sustainable Chemistry & Engineering* **2017**, *6* (1), 258–267.
- (26) Tian, J.; Li, H.; Lu, W.; Luo, Y.; Wang, L.; Sun, X. Preparation of Ag Nanoparticle-Decorated Poly(M-Phenylenediamine) Microparticles and Their Application for Hydrogen Peroxide Detection. *Analyst.* **2011**, *136* (9), 1806–1809.
- (27) Dai, S.; Peng, B.; Zhang, L.; Chai, L.; Wang, T.; Meng, Y.; Li, X.; Wang, H.; Luo, J. Sustainable Synthesis of Hollow Cu-Loaded Poly(M-Phenylenediamine) Particles and Their Application for Arsenic Removal. *RSC Advances.* **2015**, *5* (38), 29965–29974.
- (28) Li, H.; Wang, X.; Cao, L.; Zhang, X.; Yang, C. Gold-recovery PVDF Membrane Functionalized with Thiosemicarbazide. *Chem Eng J.* **2015**, *280*, 399–408.
- (29) Wang, L.; Rehman, D.; Sun, P. F.; Deshmukh, A.; Zhang, L.; Han, Q.; Yang, Z.; Wang Z.; Park, H. D.; Lienhard, J. H.; Tang, C. Y. Novel Positively Charged Metal-Coordinated Nanofiltration Membrane for Lithium Recovery. *ACS Appl Mater Inter.* **2021**, *13* (14), 16906–16915.
- (30) Zhang, L.; Wang, H.; Yu, W.; Su, Z.; Chai, L.; Li, J.; Shi, Y. Facile and Large-Scale Synthesis of Functional Poly(M-Phenylenediamine) Nanoparticles by Cu²⁺-Assisted Method with Superior Ability for Dye Adsorption. *J. Mater. Chem.C.* **2012**, *22* (35), 18244–18251.
- (31) Begum, R.; Farooqi, Z. H.; Ahmed, E.; Naseem, K.; Ashraf, S.; Sharif, A.; Rehan, R.

- Catalytic Reduction of 4-Nitrophenol Using Silver Nanoparticles-Engineered Poly(N-isopropylacrylamide-co-Acrylamide) Hybrid Microgels. *Appl Organomet Chem.* **2017**, *31* (2), 1–8.
- (32) Chai, L.; Wang, T.; Zhang, L.; Wang, H.; Yang, W.; Dai, S.; Meng, Y.; Li, X. A Cu–m-phenylenediamine Complex Induced Route to Fabricate Poly(m-phenylenediamine)/Reduced Graphene Oxide Hydrogel and Its Adsorption Application. *Carbon.* **2015**, *81*, 748–757.
- (33) Feng, B.; Yao, C.; Chen, S.; Luo, R.; Liu, S.; Tong, S. Highly Efficient and Selective Recovery of Au(III) from A Complex System by Molybdenum Disulfide Nanoflakes. *Chem. Eng. J.* **2018**, *350*, 692–702.
- (34) Liu, F.; You, S.; Wang, Z.; Liu, Y. Redox-Active Nanohybrid Filter for Selective Recovery of Gold from Water. *ACS ES&T Engineering.* **2021**, *1* (9), 1342–1350.
- (35) Chen, Z.; Wang, D.; Feng, S.; Liu, H. An Imidazole Thione-Modified Polyhedral Oligomeric Silsesquioxane for Selective Detection and Adsorptive Recovery of Au(III) from Aqueous Solutions. *ACS Appl Mater Inter.* **2021**, *13* (20), 23592–23605.
- (36) Bratskaya, S.; Privar, Y.; Ustinov, A.; Azarova, Y.; Pestov, A. Recovery of Au(III), Pt(IV), and Pd(II) Using Pyridylethyl-Containing Polymers: Chitosan Derivatives vs Synthetic Polymers. *Ind. Eng. Chem. Res.* **2016**, *55* (39), 10377–10385.
- (37) Guo, J.; Fan, X.; Wang, J.; Yu, S.; Laipan, M.; Ren, X.; Zhang, C.; Zhang, L.; Li, Y. Highly Efficient and Selective Recovery of Au(III) from Aqueous Solution by Bisthiourea Immobilized UiO-66-NH₂: Performance and Mechanisms. *Chem. Eng. J.* **2021**, *425*, 130588.
- (38) Yao, C.; Chen, S.; Wang, L.; Deng, H.; Tong, S. Low Cost and Rapid Fabrication of Copper Sulfides Nanoparticles for Selective and Efficient Capture of Noble Metal Ions. *Chem. Eng. J.* **2019**, *373*, 1168–1178.
- (39) Chen, Z.; Wang, D.; Feng, S.; Liu, H. An Imidazole Thione-Modified Polyhedral Oligomeric Silsesquioxane for Selective Detection and Adsorptive Recovery of Au(III) from Aqueous Solutions. *ACS Appl Mater Inter.* **2021**, *13* (20), 23592–23605.
- (40) Ogata, T.; Nakano, Y. Mechanisms of Gold Recovery from Aqueous Solutions Using A Novel Tannin Gel Adsorbent Synthesized from Natural Condensed Tannin. *Water Res.* **2005**, *39* (18), 4281–4286.
- (41) Hsu, E.; Barmak, K.; West, A.; Park, A. H. Advancements in The Treatment and Processing of Electronic Waste with Sustainability: A Review of Metal Extraction and Recovery Technologies. *Green Chem.* **2019**, *21*, 919–936.
- (42) Gasper, J. D.; Aiken, G. R.; Ryan, J. N. A Critical Review of Three Methods Used for The Measurement of Mercury (Hg²⁺)-Dissolved Organic Matter Stability Constants. *Appl. Geochemistry.* **2007**, *22* (8), 1583–1597.
- (43) Rajskey, T.; Urban, M. Au_n (n = 1,11) Clusters Interacting With Lone-Pair Ligands. *J Phys Chem A.* **2016**, *120* (22), 3938–3949.
- (44) Gallagher, N.; Hendrix, J.; Milosavljevic, E.; Nelson, J.; Solujic, L. Affinity of Activated Carbon Towards Some Gold (I) Complexes. *Hydrometallurgy*, **1990**, *25*, 305–316.
- (45) Liu, Y.; Zheng, Y.; Du, B.; Nasaruddin, R.; Chen, T.; Xie, J. Golden Carbon Nanotube Membrane for Continuous Flow Catalysis. *Ind. Eng. Chem. Res.* **2017**, *56*, 2999–3007.
- (46) Yazdani, H.; Hooshmand, S. E.; Varma, R. S. Gold Nanoparticle-Catalyzed Multicomponent Reactions. *ACS Sustain Chem Eng.* **2021**, *9* (49), 16556–16569.
- (47) Wang, Y.; Shi, D.; Tao, S.; Song, W.; Wang, H.; Wang, X.; Li, G.; Qiu, J.; Ji, M. A General, Green Chemistry Approach for Immobilization of Inorganic Catalysts in Monolithic Porous Flow-Reactors. *ACS Sustain Chem Eng.* **2015**, *4* (3), 1602–1610.

